

Fabrication of glutathione-modified gold nanoparticles as 3-chloropropane-1,2-diol sensor

Yora Faramitha^a, Fadhlurrahman Rafi Barori^b, Firda Dimawarnita^a, Siswanto^a, Havid Aqoma^{c,d}
Adam Febriyanto Nugraha^b, Alfian Ferdiansyah^{b,e,*}

^aIndonesian Oil Palm Research Institute–Bogor Unit, Bogor 16128, Indonesia

^bDepartment of Metallurgical and Materials Engineering, Faculty of Engineering, Universitas Indonesia, Depok 16424, Indonesia

^cKelip-kelip!, Center of Excellence for Light Enabling Technologies, School of Energy and Chemical Engineering, Xiamen University Malaysia, Selangor 43900, Malaysia

^dEnergy Conversion & Storage (EnerGONS) Group, School of Energy and Chemical Engineering, Xiamen University Malaysia, Selangor 43900, Malaysia

^eTropical Renewable Energy Center, Faculty of Engineering, Universitas Indonesia, Depok 16424, Indonesia

Article history:

Received: 28 March 2023 / Received in revised form: 15 June 2023 / Accepted: 22 June 2023

Abstract

Refined palm oil products may contain a harmful substance called as 3-monochloropropane-1,2-diol (3-MCPD), which can potentially be carcinogenic if consumed in excess. The determination of 3-MCPD depends on the sophisticated machine and highly skilled technicians but it is time-consuming. A simple method that proposes rapid detection remains a challenge. Hence, this research aims to develop a colorimetric-based rapid detection sensor using gold nanoparticles functionalized with a ligand, glutathione (GSH) to be bound to 3-MCPD. Varied concentrations of GSH were evaluated to obtain stable GSH-AuNPs. The characterization results showed that the composition of the stable GSH-AuNPs has been achieved by 250 μ L of 0.02 M GSH addition. A stable GSH-AuNPs was ruby red with surface plasmon resonance (SPR) band at 520 nm and an average nanoparticle size of 30 nm. The indication for detection of 3-MCPD was marked by the decrease in the absorbance intensity. Thus, GSH-AuNPs have potential to be developed for the 3-MCPD sensor application.

Keywords: AuNPs; ligand; 3-MCPD

1. Introduction

Palm oil is the leading agricultural commodity in Indonesia. According to the Directorate General of Estate [1], the total land area used for this commodity reached 14,586,597 hectares in 2020. As a result, various processed palm oil products became the largest export crop commodity with an export value of US\$ 18.44 billion of the total value of Indonesia's exports of US\$ 163,191.8 million [2]. In other words, palm oil products contribute to around 11.3 % of the entire export income country.

However, in the last decades, the palm oil industry has been facing a number of negative issues related to the contaminant 3-monochloropropane dienol (3-MCPD) content in refined palm oil and its derivatives. This contaminant is formed while refining crude palm oil (CPO) to become refined, bleached, deodorized palm oil (RBDPO), especially during the deodorization stage [3]. Deodorization removes free fatty acids, colors, odors, and volatile compounds from oil by distillation at a pressure in the range of 1.5 to 6.0 mbar

and high temperature in the range of 180 to 270°C [4]. The heating process at high temperatures triggers the formation of 3-MCPD compounds with the main precursors being chlorinated compounds and acylglycerols [5].

International Agency for Research on Cancer categorizes the 3-MCPD compound as Group 2B, which is possibly carcinogenic to humans based on animal testing [6]. According to food safety authorities in Europe, the limit that the human body can tolerate in consuming 3-MCPD is two ppm of body mass [7]. An excess of 3-MCPD in the body may induce various diseases, particularly kidney and testicular problems [8].

The above health problems have prompted researchers to investigate how 3-MCPD can be detected in foods. The extensively developed analytical methods for accurate 3-MCPD detection and quantification are based on Gas Chromatography-Mass Spectrometry (GC-MS) [9–11]. Other analytical methods are based on liquid chromatography-mass spectrometry/mass spectrometry (LC-MS/MS) and high-performance liquid chromatography (HPLC) [12,13]. These methods provide correct and precise analytical results. Still, these methods have several drawbacks, such as being time-consuming, complex, and dependent upon sophisticated

* Corresponding author.

Email: alfian@eng.ui.ac.id

<https://doi.org/10.21924/cst.8.1.2023.1167>

instruments and technician reliability. Hence, a simple method that proposes a rapid detection remains a challenge.

Over the past few years, metal nanoparticles have also been extensively researched and used as sensors in food safety; for example, gold nanoparticles application to detect heavy metals, pesticide residues, pathogens, and illegal additives [14]. The detection has been based on the color changes and shifts in the plasmon absorption spectra of nanoparticles. Metal nanoparticles can be synthesized using chemical reduction or green synthesis methods [15-17]. Gold nanoparticles can be chemically synthesized by tetrachloroauric acid reduction and are modified with specific ligands, such as amino acids, to be selective in detecting certain compounds or pathogens. Raj et al. (2015) [18] reported that gold nanoparticles modified with cysteine could detect *E. coli* bacteria marked by the color change from red to blue. Feng et al. (2018) [19] reported that gold nanoparticles functionalized with glutathione could detect Pb^{2+} ions, a heavy metal pollutant bringing adverse health effects on human.

A new simple and rapid test to detect free 3-MCPD has been recently reported by Martin et al. (2021) [20] by using cysteine-modified silver nanoparticles. In theory, the chlorine atom of 3-MCPD substitutes with the amine group of cysteine to form N-(2, 3 dihydroxy propyl)-amino acid grafted on AgNPs. This binding occurs by heating the mixture solution at 100°C and in an alkaline condition, as marked by the color change of the solution from yellow to pink. In this work, we proposed the use of the functionalized gold nanoparticles as a 3-MCPD sensor. Several factors contributed to the choice of gold nanoparticles, including the sensitive surface plasmon resonance and the unique optical and electrochemical properties, determined by the particles' shape, size, and aggregation state [14]. Functionalization is achieved by using glutathione as a ligand for stabilizing the nanoparticles. Glutathione has six functional groups such as amide, amine, carboxylic, and sulfhydryl. Here, sulfhydryl can bind and stabilize gold nanoparticles. Meanwhile, the amine group will substitute with the chlorine of 3-MCPD so that 3-MCPD is expected to be detected.

2. Materials and Methods

2.1. Materials

Analytical grade chemicals used for nanoparticle synthesis and colorimetric detection including tetrachloroauric acid trihydrate ($HAuCl_4 \cdot 3H_2O$), trisodium citrate dihydrate ($Na_3H_6C_5O_7 \cdot H_2O$), L-glutathione (GSH), and 3-monochloropropane-1,2-diol (3-MCPD) were purchased from Sigma-Aldrich. Deionized water with resistivity $>1 \text{ M}\Omega \cdot \text{cm}$ from the Milli-DI system was used to prepare all solutions in these experiments.

2.2. Synthesis of glutathione-modified gold nanoparticles

Gold nanoparticles were synthesized by tetrachloroauric

acid reduction with trisodium citrate, according to Devi et al. (2016) [21]. 100 mL of deionized water was heated at 90°C and 250 μL of 0.1 M tetrachloroauric acid trihydrate solution was added while vigorously stirring the DI water was at 600 rpm. Then, 2.5 mL of 0.038 M trisodium citrate was added. The mixture solution was continuously stirred and heated for 10 minutes. The change of colorless solution into a ruby red color indicated gold nanoparticle formation. The solution was then stored at room temperature overnight before any further use.

Glutathione-modified gold nanoparticles (GSH-AuNPs) were prepared by adding the different volumes of 0.02 M L-Glutathione (varied at 250, 500, and 1000 μL) to 10 mL of gold nanoparticles. The mixture was shaken by hand to ensure the glutathione was bound to AuNPs.

2.3. Characterization

The stability of GSH-AuNPs was visually documented from day 1 to day 3. The UV-vis spectra of GSH-AuNPs were recorded at a 400-800 nm wavelength range using UV-Vis Spectrophotometer (UV-Visible Multiskan Go Microplate, Thermo Scientific). The particle size distribution of GSH-AuNPs one day after synthesis was measured using a Particle Size Analyzer (PSA) (Horiba SZ 100z, ILRC Universitas Indonesia). The Fourier Transform Infrared Spectroscopy (FTIR) spectra of Glutathione and GSH-AuNPs at wave number of 400-4000 cm^{-1} were recorded using Nicolet Is5-iD7 (Thermo Scientific, Chemical Engineering Department, Universitas Indonesia).

2.4. 3-MCPD colorimetric detection experiment

A 920 μL AuNPs solution was prepared in a 2 mL microtube and 3-MCPD was added to the AuNPs solution with the various concentration of 1, 2 and 3 ppm. Next, 23 μL GSH was added, followed by DI water until the final working volume became 1 mL. This mixture was mixed by using vortex homogenization for 1 minute. The color change was observed, and this mixture's absorbance was recorded using a UV-Vis spectrophotometer.

3. Results and Discussion

Stable GSH-AuNPs must be achieved before the sensing test. Figure 1 shows the stability of GSH-AuNPs at different GSH concentrations from day one to day three. The AuNPs solution without GSH addition was stable, indicated by the similar absorbance peaks at 518 nm and no color changes in AuNPs (Figure 1(a)). On the contrary, the GSH concentration could affect the stability of gold nanoparticles. Different absorbance patterns from day one to day three were observed due to the varying concentrations of GSH. Besides, the higher the concentration of GSH, the faster the gold nanoparticle solution changed color to dark purple and, finally, colorless.

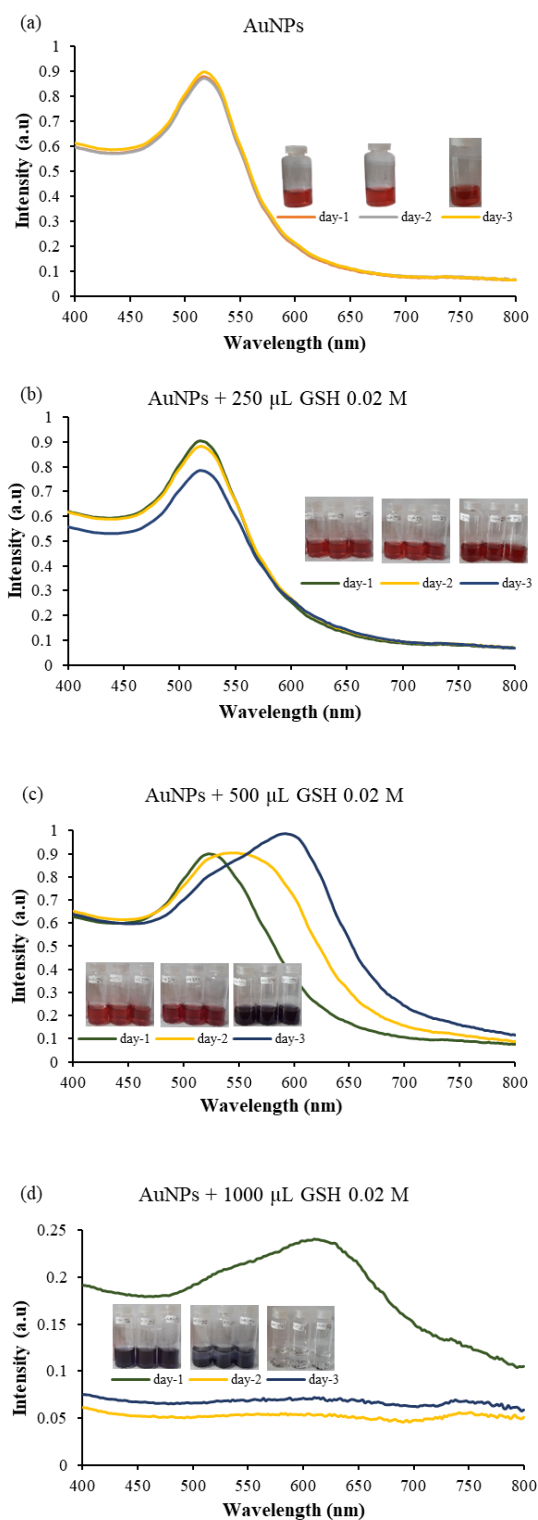


Fig. 1. Stability of gold nanoparticles added by various volumes of 0.02 M GSH: (a) 0 μL , (b) 250 μL , (c) 500 μL , and (d) 1000 μL on day 1, day 2, and day 3. Each treatment consisted of 3 replications.

Figure 1(b) shows that at the addition of 250 μL of 0.02 M GSH, the absorbance peaks slightly decreased from 0.9054 on day one to 0.8811 on day two and to 0.7862 on day three. However, the maximum absorbance remained at 518 nm. Besides, the GSH-AuNPs solution remained ruby red until day three, indicating being relatively stable. At the addition of 500 μL of 0.02 M GSH, the peak shifted to the right and

became broad (Figure 1 (c)). The absorbance peaks changed from 522 nm on day one to 542 nm on day two and to 592 nm on day three. Also, the color of the GSH-AuNPs solution changed to dark purple on day three, indicating the aggregation of gold nanoparticles. Furthermore, at the addition of 1000 μL of 0.02 M GSH, a low, broad peak was shown on day one, while no peaks were shown on day two and day three (Fig. 1(d)). The color of the gold nanoparticles solution fast changed to dark purple on day one and then became precipitate on day two. Finally, the solution became colorless on day three. Based on these results, a stable GSH-AuNPs functionalized with 250 μL of 0.02 M GSH was selected for further colorimetric detection stage.

UV-Vis spectrum patterns as shown in Figure 1 supported the color change phenomenon of GSH-AuNPs in explaining the degree of AuNPs aggregation at the different concentrations of GSH. According to Basu & Pal (2007) [22], AuNPs functionalized with GSH may result in various colors ranging from ruby red to purple to blue, reflecting the aggregation degree of AuNPs. Acres et al. (2014) [23] reported that the mixture of AuNPs and 0.01 M GSH with a ratio of 1:1 resulted in an immediate color change to dark blue, even without pH modification. These results have shown that the higher concentration of GSH could induce the aggregation of gold nanoparticles.

The stable GSH-AuNPs could be achieved due to the electrostatic repulsion between the negative charges of carboxylic groups of GSH in the form of zwitterions and the negative charges of AuNPs that may lead to weaker hydrogen bonding interactions [24]. On the other hand, the aggregation of AuNPs at higher GSH concentrations could be explained by high intramolecular hydrogen bonding among carboxyl groups of GSH and zwitterionic interaction, mainly between the thiols and the AuNPs [25–27].

Figure 2 shows the nanoparticle size distributions of GSH-AuNPs one day after synthesis based on the dynamic light scattering method. The size of nanoparticles at the addition of three different types of GSH concentrations showed an increase in particle size as the GSH concentration increased. A stable ruby red GSH-AuNPs with 250 μL GSH 0.02 M addition had an average size of 30 nm. At 500 μL GSH 0.02 M addition, a purplish red GSH-AuNPs had an average size two times larger, 65 nm. Meanwhile, at 1000 μL GSH 0.02 M addition, the particle size of purple GSH-AuNPs was about 100 nm.

The FTIR result of GSH-AuNPs as presented in Figure 3 showed a band with a 2514.88 cm^{-1} located in the band range of 2600–2550 cm^{-1} , indicating S-H stretching bonds or the thiol functional group in glutathione. Then, a peak of 1592.28 cm^{-1} located in the band range 1610–1550 cm^{-1} , representing the COO- carboxylate group, and a peak of 3337 cm^{-1} located in the band range 3650–3250 cm^{-1} , represented the functional group amino NH_3^+ .

GSH-AuNPs were characterized by large and wide band

peaks in the band range of 3000 to 3700 cm^{-1} indicating that the existence of amine group to be used for further reactions (Figure 4). The peak in the band range of 2534 cm^{-1} , a thiol group, disappeared, indicating that a thiol group was bound to AuNPs. The peak of 1647 cm^{-1} , an alkene group, represented the characteristic of gold nanoparticles [25].

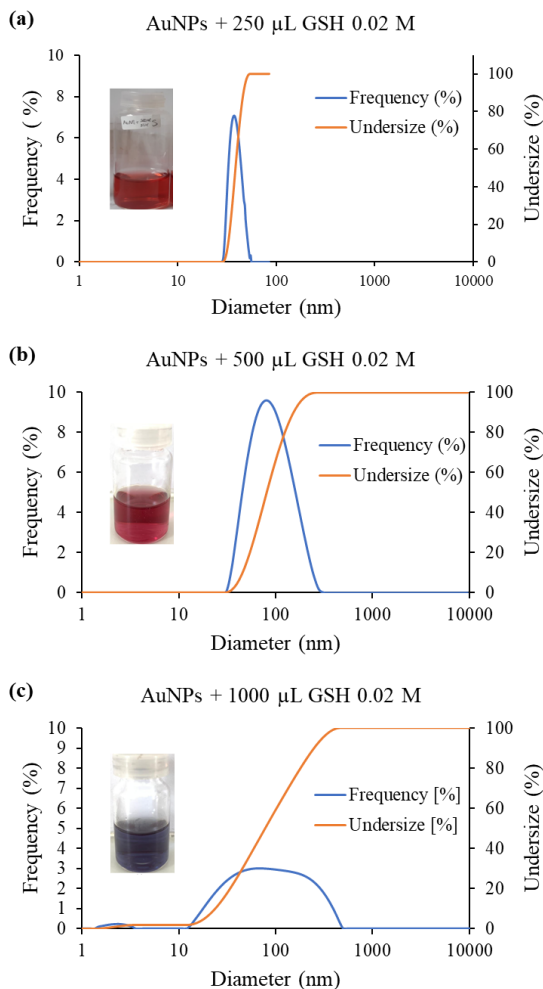


Fig. 2. Nanoparticle size distribution of gold nanoparticles added by various volumes of 0.02 M GSH: (a) 250 μL , (b) 500 μL , and (c) 1000 μL

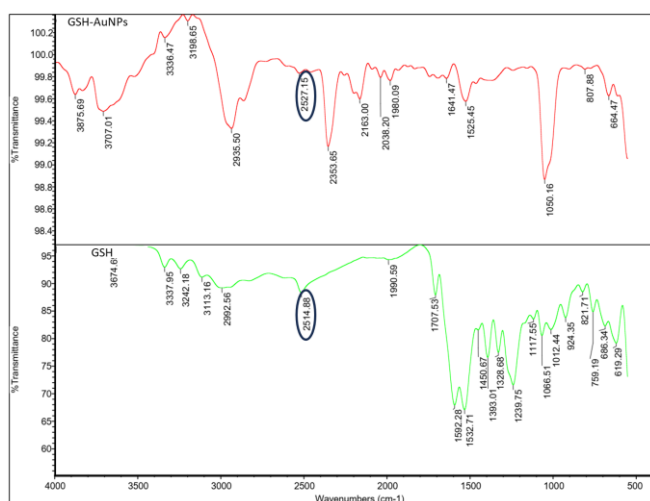


Fig. 3. FTIR characterization of (a) GSH-AuNPs and (b) GSH

absorption GSH-AuNPs with three different concentrations of 3-MCPD. It showed that although the color of GSH-AuNPs did not change along with the higher 3-MCPD concentrations, lower absorption spectra strongly indicated 3-MCPD sensing. As seen in the inset of Figure 5, the higher the 3-MCPD content, the lower the UV-Vis spectra of GSH-AuNPs. It is assumed that the chlorine atom of 3-MCPD substituted with the amine group of glutathione to form N-(2,3 dihydroxy propyl)-amino acid grafted on AuNPs, as reported by Martin et al. [20]. The schematic of proposed reaction in this work is shown in Figure 6. Hence, the gold nanoparticle has enormous potential as a sensor of 3-MCPD.

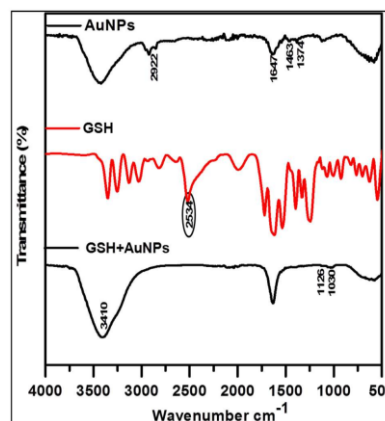


Fig. 4. FTIR spectrum of AuNPs, GSH, and GSH-AuNPs [25]

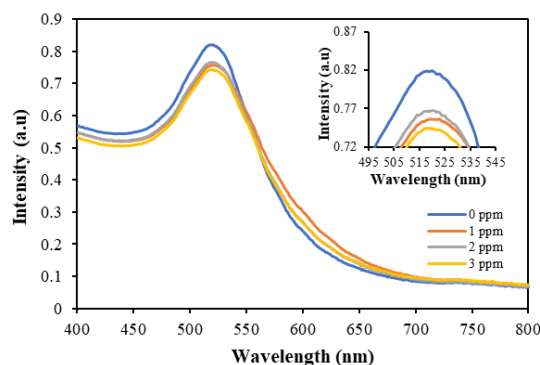


Fig. 5. UV-Vis spectrum of a stable ruby red GSH-AuNPs with 250 μL GSH 0.02 M added with various concentrations of 3-MCPD. Inset: The decreased absorption signal of GSH-AuNPs due to increasing 3-MCPD content.



Fig. 6. Schematic of proposed reaction resulting from the interaction between GSH-AuNPs and 3-MCPD.

4. Conclusion

The synthesis of glutathione-modified gold nanoparticles (GSH-AuNPs) was successfully carried out. An optimal functionalization of stable gold nanoparticles was achieved by binding to a glutathione ligand, which acted as a stabilizing

Figure 5 presents the absorption spectra of the optical

agent. The stable GSH-AuNPs had constant ruby red color and an average nanoparticle size of 30 nm. Nevertheless, GSH-AuNPs did not change color when added with 3-MCPD. A decrease in the UV absorption intensity represented a solid indication of the detection of 3-MCPD. Compared to GSH-AuNPs with the intensity peak of about 0.8197, adding three ppm of 3-MCPD lowered the intensity to 0.744. In conclusion, GSH-AuNPs have the potential to be developed in the detection of 3-MCPD applications. The further experiment can be focused on the size variation of AuNPs to increase the sensitivity of nanoparticles in detecting 3-MCPD.

Acknowledgements

This research was financially supported by The Indonesian Palm Oil Plantation Fund Management Agency (BPDPKS), contract number PRJ-24/DPKS/2021. We also thank for partly support from Hibah Publikasi Terindeks Internasional (PUTI Q2) contract number NKB-797/UN2.RST/HKP.05.00/2023. Finally, we thank to Khairy Yunda Maharani who helped in carrying out the research activities.

References

1. Directorate General of Estate, *Statistical of National Leading Estate Crops Commodity 2020-2022*, 2022.
2. BPS, *Indonesia Foreign Trade Statistics Exports 2020*, 1, 2021.
3. K. Hrnčirik and G. van Duijn, *An initial study on the formation of 3-MCPD esters during oil refining*, Eur. J. Lipid Sci. Technol. 113 (2011) 374–379.
4. CODEX, *Code of practice the reduction of 3-MCPDs and GEs in refined oils and food products made with refined oils*, 2019.
5. A. Ermacorà and K. Hrnčirik, *Influence of oil composition on the formation of fatty acid esters of 2-chloropropane-1,3-diol (2-MCPD) and 3-chloropropane-1,2-diol (3-MCPD) under conditions simulating oil refining*, Food Chem. 161 (2014) 383–389.
6. IARC Working Group on the Evaluation of carcinogenic risks to humans, *3-monochloro-1, 2-propanediol, in some chemicals present in industrial and consumer products, food and drinking-water*, International Agency for Research on Cancer 101 (2013) 349-369.
7. EFSA, *Analysis of occurrence of 3-monochloropropane-1, 2-diol (3-MCPD) in food in Europe in the years 2009-2011 and preliminary exposure assessment*, EFSA J. 11 (2013) .
8. B. Gao, Y. Li, G. Huang and L. Yu, *Fatty acid esters of 3-monochloropropanediol: a review*, Annu. Rev. Food Sci. Technol. 10 (2019) 259–284.
9. W. Kim, Y.A. Jeong, J. On, A. Choi, J.Y. Lee, J.G. Lee et al., *Analysis of 3-MCPD and 1,3-DCP in various foodstuffs Using GC-MS*, Toxicol. Res. 31 (2015) 313–319.
10. X. Zheng, W. Fu, K. Zheng, B. Gao, L. Lin, W. Liu et al., *A novel method for the simultaneous determination of esterified 2-/3-MCPD and glycidol in foods by GC-MS/MS*, Food Control. 123 (2021) 107766.
11. Z.A. Talitha, N. Andarwulan and D.N. Faridah, *Verification of AOCS Cd 29a-13 2013 method for 3-MCPDEs (3-Chloropropane-1.2-Diol Esters) and GE (Glycidol Esters) analysis in palm oil*, Int. J. Oil Palm. 3 (2020) 11–22.
12. K. Yamazaki, M. Ogiso, S. Isagawa, T. Urushiyama, T. Ukena and N. Kibune, *Food Additives & Contaminants: Part A A new , direct analytical method using LC-MS / MS for fatty acid esters of 3-chloro-1 , 2-propanediol (3-MCPD esters) in edible oils*, Food Addit. Contam. 30 (2013) 52–68.
13. H. Zhou, Q. Jin, X. Wang and X. Xu, *Direct measurement of 3-chloropropane-1,2-diol fatty acid esters in oils and fats by HPLC method*, Food Control. 36 (2014) 111–118.
14. Z. Hua, T. Yu, D. Liu and Y. Xianyu, *Recent advances in gold nanoparticles-based biosensors for food safety detection*, Biosens. Bioelectron. 179 (2021) 113076.
15. M.H. Husein, N.F. Abu Bakar, A.N. Mustapa, K.F. Low, N.H. Othman and F. Adam, *Synthesis of various size gold nanoparticles by chemical reduction method with different solvent polarity*, Nanoscale Res. Lett. 15 (1) (2020) 1-10.
16. A. Chafidz, A.R. Afandi, B.M. Rosa, J. Suhartono, P. Hidayat and H. Junaedi, *Production of silver nanoparticles via green method using banana raja peel extract as a reducing agent*, Commun. Sci. Technol. 5 (2) (2020) 112-118.
17. N. Munandar, S. Kasim, R. Arfah, D.N. Basir, Y. Hala., M. Zakir and H. Natsir, *Green synthesis of copper oxide (CuO) nanoparticles using Anredera cordifolia leaf extract and their antioxidant activity*, Commun. Sci. Technol. 7 (2) (2022) 127-134.
18. V. Raj, A.N. Vijayan and K. Joseph, *Cysteine capped gold nanoparticles for naked eye detection of E. coli bacteria in UTI patients*, Sens. Bio-Sensing Res. 5 (2015) 33–36.
19. B. Feng, R. Zhu, S. Xu, Y. Chen and J. Di, *A sensitive LSPR sensor based on glutathione-functionalized gold nanoparticles on a substrate for the detection of Pb²⁺ ions*, RSC Adv. 8 (2018) 4049–4056.
20. A.A. Martin, E.K. Fodjo, G.B.I. Marc, T. Albert and C. Kong, *Simple and rapid detection of free 3-monochloropropane-1,2-diol based on cysteine modified silver nanoparticles*, Food Chem. 338 (2021) 127787.
21. S. Devi, B. Singh, A.K. Paul and S. Tyagi, *Highly sensitive and selective detection of trinitrotoluene using cysteine-capped gold nanoparticles*, Anal. Methods. 8 (2016) 4398–4405.
22. S. Basu and T. Pal, *Glutathione-induced aggregation of gold nanoparticles: Electromagnetic interactions in a closely packed assembly*, J. Nanosci. Nanotechnol. 7 (2007) 1904–1910.
23. R.G. Acres, V. Feyer, N. Tsud, E. Carlino and K.C. Prince, *Mechanisms of aggregation of cysteine functionalized gold nanoparticles*, J. Phys. Chem. C 118 (2014) 10481–10487.
24. M.R. Hormozi-Nezhad, E. Seyedhosseini and H. Robotjazi, *Spectrophotometric determination of glutathione and cysteine based on aggregation of colloidal gold nanoparticles*, Sci. Iran. 19 (2012) 958–963.
25. R. Manjumeena, D. Duraibabu, T. Rajamuthuramalingam, R. Venkatesan and P.T. Kalaichelvan, *Highly responsive glutathione functionalized green AuNP probe for precise colorimetric detection of Cd²⁺ contamination in the environment*, RSC Adv. 5 (2015) 69124–69133.
26. I.I.S. Lim, D. Mott, W. Ip, P.N. Njoki, Y. Pan, S. Zhou et al., *Interparticle interactions in glutathione mediated assembly of gold nanoparticles*, Langmuir. 24 (2008) 8857–8863.
27. Z.A. Tehrani, Z. Jamshidi, M.J. Javan and A. Fattahi, *Interactions of glutathione tripeptide with gold cluster: Influence of intramolecular hydrogen bond on complexation behavior*, J. Phys. Chem. A 116 (2012) 4338–4347.